Journal of the European Ceramic Society 22 (2002) 93–99

www.elsevier.com/locate/jeurceramsoc

Nanometer silicon carbide powder synthesis and its dielectric behavior in the GHz range

Bo Zhang[a,*], Jianbao Li[a], Jingjing Sun[a], Shuxia Zhang[a], Huazhang Zhai[a], Zhengwei Du[b]

[a]*State Key Laboratory of New Ceramics and Fine Processing, Department of Materials Science and Engineering, Tsinghua University, Beijing 100084, PR China*

[b]*Department of Electronic Engineering, Tsinghua University, Beijing 100084, PR China*

Received 12 October 2000; received in revised form 21 February 2001; accepted 4 March 2001

Abstract

In this paper, the dielectric properties of nano-sized SiC powders have been investigated in the GHz frequency range. The polytypes of SiC have been changed from β type (3C) to α type (12H and 21R) by varying the aluminum contents and the reaction atmospheres. The β-SiC powder has much higher relative permittivity ($\varepsilon'_r = 30 \sim 50$) and loss tangent ($tg\delta = \sim 0.7$) than α-SiC powders. Though the doping of Al and N decrease the resistivity of SiC to the order of 10^2 Ω cm, the pivotal factor on the dielectric behaviors is ion jump and dipole relaxation, namely the reorientation of lattice defect pairs (V_{Si}–V_C, Si_C–C_{si}). The conductivity of SiC has little effect on the dielectric behaviors. © 2001 Elsevier Science Ltd. All rights reserved.

Keywords: Defects; Dielectric properties; Powders; SiC; Sol-gel processes

1. Introduction

As more and more tools taking advantage of microwave come into use, such as mobile telephones, microwave ovens and so on, serious problems on the electromagnetic compatibility and radioprotection have received much attention. Many efforts have been made to develop electromagnetic wave absorption materials for the use in the GHz range.

The absorption of electromagnetic waves is either due to ohmic or to hysteresis losses in the absorbing material. Plastics loaded with carbon powder are representative of absorbers based on ohmic losses.[1] Ferrites are typical electromagnetic wave absorption materials based on hysteresis losses.[2,3] Theoretically, the former absorbers can work equally for signals with small or large relative bandwidth. In fact, they cannot be used for the signals with large relative bandwidth due to the excessive thickness required for the absorbing materials. However, hysteresis losses have a completely different effect on signals with large relative bandwidth rather than a small one. Currently available ferrites can match the impedance of free space only over a small relative bandwidth.[4,5] One can infer from the above that current absorbers are not effective for signals with large relative bandwidth and it is necessary to look for new electromagnetic wave absorbing materials, including composite materials.

Silicon carbide was studied as a structural ceramic for a long time. However, silicon carbide is also a microwave absorber.[6] In microwave processing, SiC can absorb electromagnetic energy and be heated easily. It has a loss factor of 1.71 at 2.45 GHz at room temperature. And the loss factor at 695°C for the same frequency will increase to 27.99. This ability for microwave absorption is due to the semiconductivity. In fact, SiC is a wide band gap semiconductor with many attractive properties, such as high breakdown field strength, high saturated carrier drift velocity and high thermal conductivity.[7,8] Compared with other ohmic loss absorbers, SiC has an important character in that its electrical properties can be adjusted by forming solid solutions with varieties of materials (e.g. AlN, Al_4C_3, BN, B_4C).[9,10] Compared with ferrites, SiC can be used in high temperature conditions and its loss factor will increase

* Corresponding author.
E-mail address: zhang_b@263.net (B. Zhang).

0955-2219/01/$ - see front matter © 2001 Elsevier Science Ltd. All rights reserved.
PII: S0955-2219(01)00248-5

with temperature.[6] These attractive properties make silicon carbide a promising absorber for electromagnetic wave with large relative bandwidth. By far, some works have been donated to the absorbers that consist of SiC fibers and have some developments[11–13]. Nevertheless, SiC powder is more convenient than SiC fiber when the absorbers are used as coatings. Unfortunately, there are few systematic studies on the microwave absorption properties of SiC powders though some characters have been referred to by Sutton.[6]

This paper aims to do some detail investigations on the microwave absorption properties of SiC powders. We synthesized nano-sized SiC powders (3C, 12H, 21R) and investigated the dielectric parameters in GHz range, such as relative permittivity and loss tangent. The powders phase component and morphology were studied with XRD and TEM, respectively.

2. Experimental procedure

The nano-sized SiC powders were synthesized with carbothermal reduction of SiO_2 and SiO_2–Al_2O_3 xerogels. For the SiO_2–Al_2O_3 xerogels, the initial mixture sol was prepared by mixing 100 ml of TEOS (tetraethylorthosilicate), 30 ml of ethanol, 100 ml of water, 50 g of saccharose ($C_{12}H_{22}O_{11}$) and some Al_2O_3 powders. The alumina particles possessed a middle diameter of 0.2 μm. The content of Al_2O_3 was varied in order to study the effect of Al on the phase and microwave absorptivity of SiC powders. The detailed compositions of samples are listed in Table 1. During the stirring, the value of pH was kept at 4.5 with the addition of HNO_3. After being stirred for 4 h, the mixture sol was allowed to gel, age and dry at 40°C.

The xerogels of SiO_2 and SiO_2–Al_2O_3 were heated at 600°C for 2 h to carbonize the saccharose and then heated at 1550°C for 1 h in an argon or a nitrogen atmosphere to synthesize SiC (Table 1). The products obtained in these procedures were heated at 650°C in air to remove excess carbon and then treated with dilute hydrofluoric acid to remove remainder silica.

The samples for dielectric parameter measure were prepared by blending SiC powders with paraffin wax and pressing the mixture to rings with the dimension of $7.00\times3.04\times3$ mm^3 (outer diameter×inner diameter×thickness). The volume ratio of SiC powders to paraffin wax was 1:1.5. The densities of samples were kept at about 1.82 g/cm^3. The errors of densities were less than 5%.

XRD (D/MAX IIIB, Cu-K_α) was used to analyze the crystallographic composition and polytypes of carbothermal reduction products. Lattice definition was carried out with the inner 99.99% Si standard (particles size 10 μm, $a=5.43088$ Å). The compositions of powders were investigated with SEM (JSM-6301F) coupled with EDS. TEM (JEM-200CX) was adopted to observe the morphology and measure the sizes of SiC powders. The dielectric parameters were measured with Network Analyzer (HP 8510B) on the circular samples.

Table 1
The content of alumina in xerogels and different reaction atmosphere

Sample	Atom ratio of Al–Si	Reaction atmosphere
1	0	Argon
2	2.63:100	Argon
3	5.26:100	Argon
4	2.63:100	Nitrogen
5	5.26:100	Nitrogen

3. Results and discussion

3.1. The compositions of SiC powders

Fig. 1 shows the results from the EDS. In the EDS spectra of powders 2 and 3, there exist four peaks due to C, O, Al and Si, respectively, and elements of C, N, O, Al and Si exist in powders 4 and 5. Element oxygen exists in all of the five powders and is donated by the oxide surface of powders. Under many circumstances, silicon compounds possess the surface of SiO_2. The content of C, N and O cannot be determined precisely because of the limitation of EDS for light elements.

3.2. The polytypes and lattice parameters of SiC powders

The XRD spectrum of carbothermal reduction products is shown in Fig. 2. The XRD patterns indicate that there only exist the peaks belonging to SiC, which correspond to 3C, 12H and 21R. Powder 1 synthesized

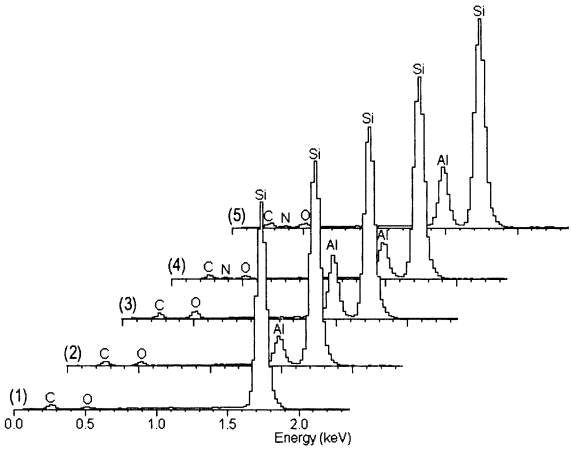

Fig. 1. The compositions of powders by EDS.

without Al_2O_3 possesses the phase of 3C (β-SiC). For the powders containing aluminum, the polytypes change to α type. In detail, powders 2 and 3, which were obtained in the atmosphere of argon, have the structure of 12H; powders 4 and 5, which were obtained in nitrogen, have the structure of 21R.

It can be noted that the 002 reflection is hardly observed in powder 1. This case can be explained with the appearance of the $d=2.65$ Å reflection, which indicates that the presence of stacking faults in the β-SiC structure. It was shown by simulation by Tateyama et al. [14] that the stacking faults in the structure of β-SiC led to the synchronous diffraction effects: arising from additive reflection of $d=2.65$ Å, and a reduction of integral intensity of 002 reflection. The precise lattice parameter test determines the $a=4.341$ Å, which is 0.018 Å smaller than the standard value of 4.3589 Å. The smaller lattice parameter is due to the partial substitution of silicon atoms by carbon atoms having a smaller covalent radius.

The powders containing aluminum have the α structure. The changes in crystalline are led to by the addition of aluminum and nitrogen. During the synthesis of silicon carbide, Al_2O_3 is reduced by carbon and forms carbide. At the same time, aluminum dopes into SiC and forms solid solution. Aluminum atoms replace atoms of silicon in the solid solution and induce vacancies of carbon. As a result of the substitution, reflection of (103) emerges as well as the reflection of (101). As the content of aluminum increases, the relative intensities of the reflection of (103) and (101) also rise. However, the rising of the reflection of (103) is finite. Though aluminum has a larger atom radius than silicon, and consequently, should make the lattice expand, the vacancy of carbon could lead the lattice to shrink more. These two effects counteract and reduce the lattice parameters as a whole. The lattice parameters are listed in Table 2, in which a and c decrease with the increasing of aluminum content.

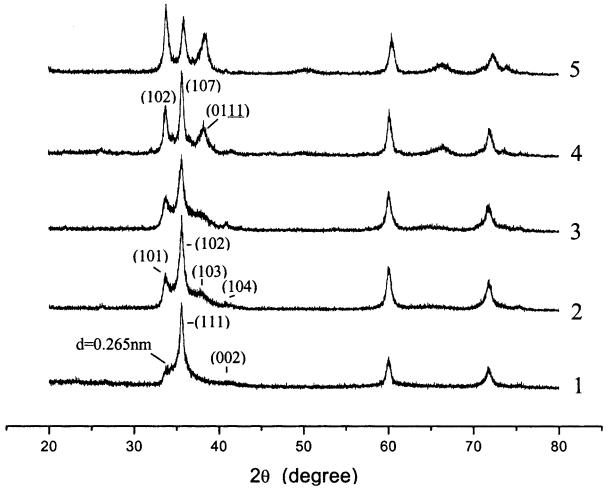

Fig. 2. X-ray diffraction patterns of SiC powders.

Powders 4 and 5 possess the polytype of 21R. At the same time, these powders have much larger shrinkage in lattice than those powders synthesized in argon. This large shrinkage in lattice is due to the formation of silicon vacancies in lattice. When SiC powders are synthesized in an atmosphere of nitrogen, nitrogen atoms replace some carbon atoms and form silicon vacancies.

3.3. The size and morphology of SiC powders

In the XRD patterns, all peaks are broadened because of the ultrafine crystals. The grain sizes of samples can be estimated with the Scherrer formula:

$$D_{hkl} = k\lambda/(B_{1/2}\cos\theta), \quad (1)$$

where the D_{hkl} is the grain size in the direction perpendicular to the crystal face {hkl}, k is a constant of Scherrer, λ is the wavelength of X-ray, $B_{1/2}$ is the broadness at half high of the peak, and θ is the Bragg angle of crystal face {hkl}. After broadening due to the apparatus has been deducted, the grain sizes of powders are calculated and listed in Table 2. For all of the powders, the grain sizes are in the range of 13–20 nm.

Fig. 3 shows the TEM images of SiC powders. The powders show very fine equiaxial crystallites with the diameters of about 20 nm. Though this result corresponds to the XRD analysis, the sizes of powders 1 and

Table 2
The lattice of nanometer-sized silicon carbide

Powder	Crystalline structure	Grain size (nm)	Standard Lattice (Å)	Tested Lattice (Å)
1	β(3C)	18.3	$a=4.3589$	$a=4.341$
2	12H	15.2	$a=3.073$	$a=3.070$
			$c=15.080$	$c=15.036$
3	12H	12.9	$a=3.073$	$a=3.062$
			$c=15.080$	$c=14.999$
4	21R	19.4	$a=3.073$	$a=3.049$
			$c=52.78$	$c=52.336$
5	21R	15.2	$a=3.073$	$a=3.026$
			$c=52.78$	$c=51.921$

2 are seemingly larger than the calculated values. This difference is due to the agglomeration of powders. Additionally, XRD analysis is a statistical result and will make the diameters of powders differ from the diameters directly measured from the TEM images unless the powders have the same size. The TEM images can only reflect the morphology of partial powders. The agglomeration hinders correct evaluation of the particle sizes by ordinary techniques such as LPS (laser particle sizer).

3.4. The dielectric behaviors of SiC powders

Fig. 4 gives the relative permittivities (ε'_r) and loss tangents ($tg\delta$) of SiC powders in the range of 8.2–12.4 GHz. Sample 1 (β-SiC) has the highest relative permittivity and loss tangent in the powders. For the samples with Al, the relative permittivities and loss tangents are in an inverse measure of the content of aluminum. For the powders with the same aluminum content, the samples synthesized in nitrogen atmosphere have smaller values for ε'_r and $tg\delta$ than those obtained in argon atmosphere. With the increase of frequency, all the curves have only minute changes.

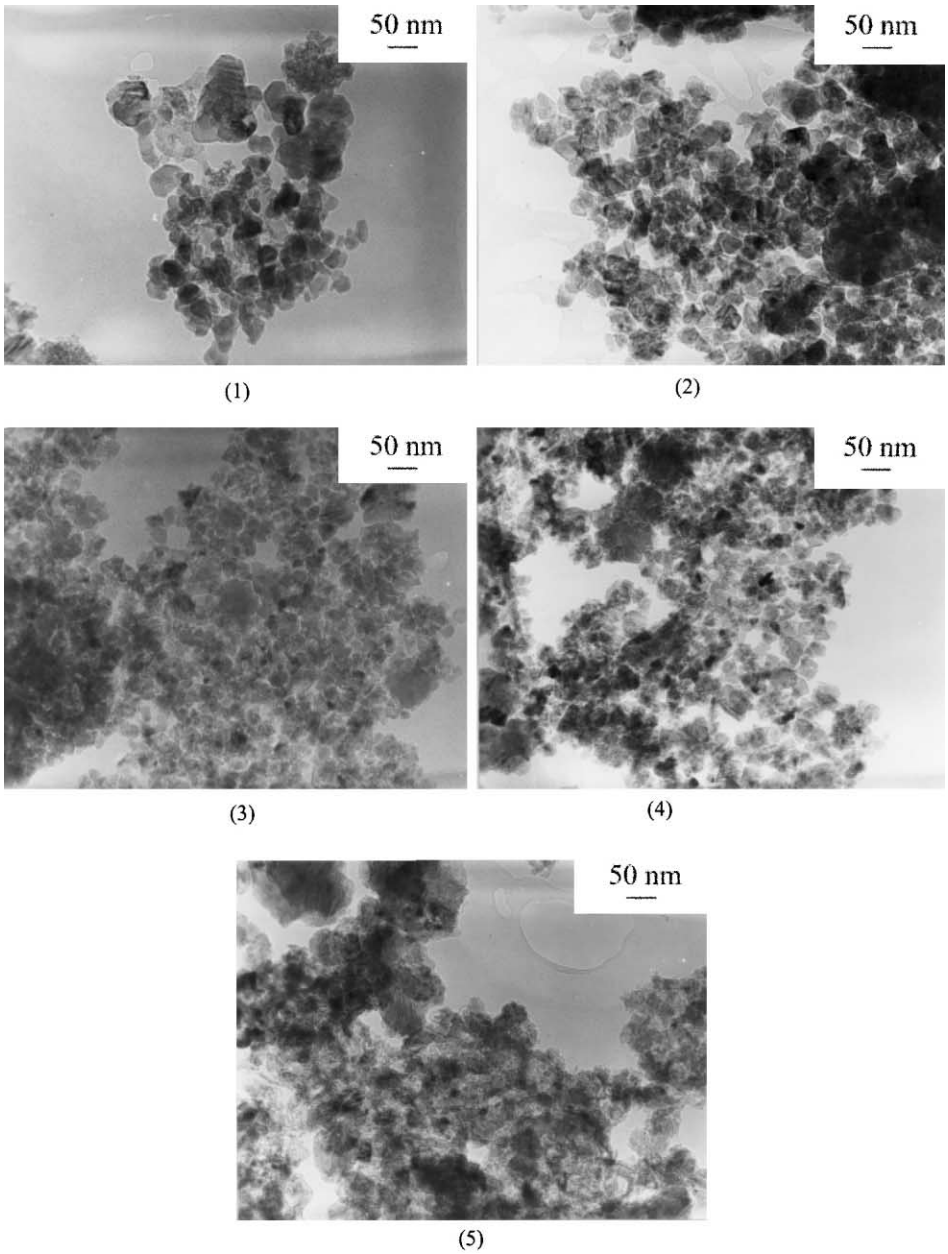

Fig. 3. The morphology of SiC powders by TEM.

Because the relative permeability (μ'_r) of silicon carbide is equal to 1, the power dissipation is only determined by dielectric losses. Dielectric losses usually consist of ion migration losses [including (a) DC conductivity losses and (b) ion jump and dipole relaxation losses], ion vibration and deformation losses, and electron polarization losses. For the polycrystalline and polyphase materials, the losses due to the space charge polarization must be considered. The electron polarization losses give rise to absorption and color in the visible spectrum. The ion vibration and deformation losses become important in the infrared. When the frequency is below about 10^{10} Hz, only the rest energy loss mechanisms determine the dielectric losses. Therefore, the loss tangent can be expressed as follows:

$$tg\delta = \frac{\varepsilon''_C + \varepsilon''_R + \varepsilon''_I}{\varepsilon'} \tag{2}$$

where ε''_C is the loss factor due to conductivity, ε''_R is the one due to ion jump and dipole relaxation, and ε''_I is the one due to space charge polarization.

DC conductivity losses are important for many dielectric materials. Therefore, it must be considered first. In the samples with aluminum, aluminum and nitrogen atoms will substitute Si and C atoms, respectively. Except the native defect reactions, the following defect reactions would happen:

$$Al \xrightarrow{SiC} Al'_{Si} + h^{\cdot} \tag{3}$$

$$Al_4C_3 \xrightarrow{SiC} 4Al'_{Si} + 3C_C + V_C^{\cdots\cdot} \tag{4}$$

$$N \xrightarrow{SiC} N_C^{\cdot} + e' \tag{5}$$

$$AlN \xrightarrow{SiC} Al'_{Si} + N_C^{\cdot} \tag{6}$$

$$Al_2O_3 \xrightarrow{SiC} 2Al'_{Si} + 3O_C^{\cdot\cdot} + V_{Si}'''' \tag{7}$$

In detail, reactions 3, 4 and 7 have possibilities to happen in the synthesis reaction for SiC in argon atmosphere, and reactions 3, 5, 6 and 7 may exist when the SiC powders are synthesized in nitrogen atmosphere. The substitution of silicon atoms by aluminum atoms leads to an acceptor level within the band gap and the conductivity due to holes. Therefore, the conductivity of SiC powder without nitrogen simply increases with the rise of aluminum content. On the other hand, the nitrogen atoms lead to an electron donor level and the conductivity due to electrons. When both Al and N exist in SiC powders, the concentration of carriers will decrease because of the two contrary carriers. However, the drift mobility of carriers is the sum of the mobilities of these two carriers. Being a result of the higher carrier mobility, the conductivity of SiC with nitrogen is much higher than that of SiC without nitrogen. Table 3 lists the DC resistivities of SiC powders. The table indicates that the change of resistivities for the samples including Al corresponds with the above analysis, namely, the resistivities of samples 4 and 5 are lower than those of samples 2 and 3, respectively.

The increase of electrical conductivity would result in the rise of dielectric loss. In formula 2, the loss due to conductivity is as follows:

$$tg\delta_C = \frac{\varepsilon''_C}{\varepsilon'} = \frac{\sigma}{2\pi f\varepsilon'_r\varepsilon_0} = \frac{1}{2\pi f\varepsilon'_r\varepsilon_0 R} = \frac{1}{(8.85\times10^{-14})2\pi f\varepsilon'_r R}, \tag{8}$$

Table 3
The DC resistivities and calculated loss tangent[a] of SiC powders

Sample	DC resistivity (Ω cm)	Calculated loss tangent for 10 GHz
1	557.9	8.00×10^{-2}
2	1803.5	8.78×10^{-2}
3	511.3	3.57×10^{-1}
4	1181.7	1.84×10^{-1}
5	77.5	4.06×10^{-1}

[a] The values are calculated for pure SiC samples.

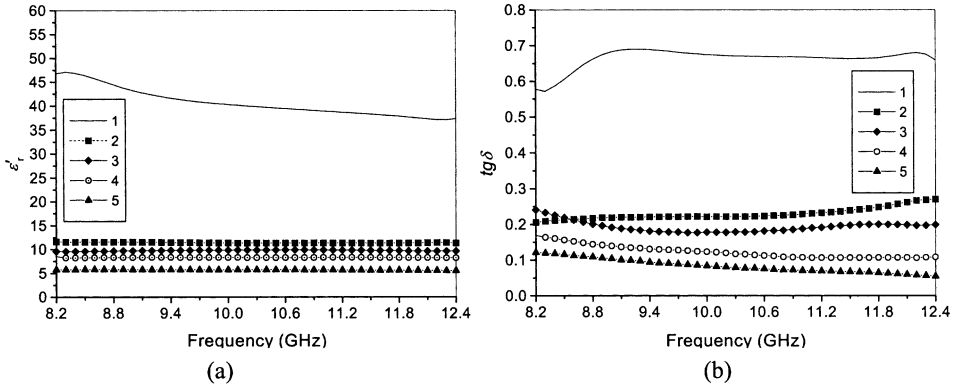

Fig. 4. The relative permittivity ε'_r (a) and loss tangent $tg\delta$ (b) of the samples consisting of SiC powders (40 vol %) and paraffin wax (60 vol %).

where the resistivity is given in Ω cm. The loss tangents for pure SiC samples for the frequency of 10 GHz are also calculated in Table 3. Here, the values of ε'_r for samples containing 40 vol.% SiC powder are simply adopted. In fact, the true value of ε'_r is much higher than the measured one and can be deduced according to the mixture rules. Therefore, the practical value of $tg\delta_c$ is lower than the calculation one. However, the loss tangents of samples 2–5 decrease with the rise of conductivities. Especially, the loss tangent of sample 1 is much higher than the loss tangent of other samples, though samples 4 and 5 have lower resistivities. All of these phenomena indicate that conductivity loss is not the main factor on the dielectric loss in the current samples.

Because the SiC powders have similar sizes and the SiC volume contents in the circular samples are the same, the space charge polarization due to the polycrystalline and polyphase should provide a similar effect on the dielectric losses. Consequently, only ion jump and dipole relaxation have the possibilities of affecting the dielectric behaviors of samples. In 3C SiC, the silicon and carbon vacancies (V_{Si}, C_{Si}) as well as silicon and carbon antisites (Si_C, V_C) are the most energetically adoptable among native SiC defects preserving a tetrahedral symmetry.[15,16] The defects with contrary charges have a strong trend to form pairs because of the static attraction. These defect pairs can be treated as dipoles. The more the dipoles, the higher the relative dielectric constant. Under the alternating electric field, the reorientation of these lattice defect pairs results in polarization and energy dissipation. In this case, a high relative dielectric constant means high dielectric loss because the reorientation must be completed by the migration of ions, which will dissipate energy. This is the reason why sample 1 possesses the high ε'_r and $tg\delta_c$. When aluminum has been doped into SiC, aluminum atoms occupy the sites of silicon atoms and deduce the number of those defect pairs. Though aluminum atoms can also partner the defects with contrary charge, it is more difficult for such defect pairs to reorientate because aluminum atoms have larger a covalent radius than silicon atoms. The number of defect pairs that can take part in polarization decreases with the rising of aluminum content. Therefore, with the rising of aluminum content, the conductivity of SiC increases, but the relative permittivity and loss tangent decrease. Nitrogen atoms act as similar roles and lead to more reduction in the relative permittivity and loss factors.

4. Conclusions

Nano sized β type (3C) and α type (12H and 2lR) SiC powders with the diameter of about 20 nm have been synthesized by carbothermal reduction of SiO_2 and SiO_2–Al_2O_3 xerogels. Aluminum and nitrogen have important affection on the polytypes of SiC powders. When there existed aluminum, the l2H SiC powders were obtained. The 21R SiC was synthesized under the nitrogen atmospheres. The decrease of lattice parameters reflects the formation of vacancy.

The β-SiC powder has much higher relative permittivity ($\varepsilon'_r = 30 \sim 50$) and loss tangent ($tg\delta = 0.7 \sim 0.9$) than all of the α-SiC powders, though the α-SiC powders with 5.26 mol% aluminum possess higher conductivities. The pivotal factor on the dielectric behaviors is ion jump and dipole relaxation, namely the reorientation of lattice defect pairs (V_{Si}–V_C, Si_C–C_{Si}). Aluminum and nitrogen decrease the defect pairs that contribute to polarization. With the increase of the aluminum content and the doping of nitrogen, the conductivity of SiC rises, but the relative dielectric constant and loss tangent decrease.

Acknowledgements

This research was supported by The Basic Research Foundation of Tsinghua University (Project No. JZ0009) and The Open Project Foundation of the State Key Laboratory of New Ceramics and Fine Processing in Tsinghua University (Project No. KF0003).

References

1. Harmuth, H. F., On the effect of absorbing materials on electromagnetic waves with large relative bandwidth. *IEEE Trans. Electromagn. Compat*. 1983, **EMC-25**, 32–39.
2. Naito, Y. and Suetaki, K., Application of ferrite to electromagnetic wave absorber and its characteristics. *IEEE Trans. Microwave Theory Technol*. 1971, **MTT-19**, 65–72.
3. Sugimoto, S., Okayamam, K., *et al*. Barium M-type ferrite as an electromagnetic microwave absorber in the GHz range. *Materials Transactions* 1998, **39**, 1080–1083.
4. Amin, M. and James, J. R., Techniques for utilization of hexagonal ferrites in radar absorbers. Part 1: broadband planar coatings.. Radio Electron. Eng. (London) 1981, **51**, 209–218.
5. James, J. R. and Amin, M. B., Techniques for utilization of hexagonal ferrites in radar absorbers. Part 2: reduction of radar cross-section of HF and VHF wire antennas. *Radio Electron. Eng. (London)* 1981, **51**, 219–225.
6. Sutton, W. H., Microwave processing of ceramics — an overview. In *Microwave Processing of Materials III*, ed. R. L. Beatty, M. F. Iskander and W. H. Sutton. Materials Research Society, San Francisco, 1992, pp. 3.
7. Morkoc, H., Strite, S. and Guo, G. B., Large-band-gap SiC, III-V nitride, and II-VI ZnSe-based semiconductor device technologies. *J. Appl. Phys*. 1994, **76**, 1363–1398.
8. Krstic, V. D., Production of fine, high-purity Beta silicon carbide powders. *J. Am. Ceram. Soc*. 1992, **75**, 170–174.
9. Inomata, Y., Tanaka, H., Inoue, Z. and Kawabata, K., Phase relation in SiC–AI_4C_3–B_4C system at 800°C. *J. Ceram. Soc. Jpn*. 1980, **88**, 353–355.
10. Ervin, G., Jr., Silicon carbide-aluminum nitride refractory composite. US Patent 3492153 27 January 1970.

11. Ishikawa, T., Recent developments of the SiC fiber nicalon and its composite, including properties of the SiC fiber hi-nicalon for ultra-high temperature. *Comp Sci. Technol.* 1994, **51**, 135–144.
12. Narisawa, M., Itoi and Okamura, Y. K., Electrical resistivity of Si–Ti–C–O fibres after rapid heat treatment. *J. Mater. Sci.* 1995, **30**, 3401–3406.
13. Yamamuna, T., Ishikawa, T. and Shibuya, M., Electromagnetic wave absorbing material. US Patent 5094907 10 March 1992.
14. Tateyama, H., Sutoh, N. and Murakawa, N., Quantitative analysis of stacking faults in the structure of SiC by X-ray powder profile refinement method. *J. Ceram. Soc. Jpn. Int. Ed.* 1988, **96**, 1003–1011.
15. Wang, C., Bernholc, J. and Davis, R. F., Formation energies, abundances, and the electronic structure of native defects in cubic SiC. *Phys. Rev. B,* 1988, **38**, 12752–12755.
16. Bernholc, J., Kajihara, S. A., Wang, C., Antonelli, A. and Davis, R. F., Theory of native defects, doping and diffusion in diamond and silicon carbide. *Mater. Sci. Eng. B,* 1992, **B11**, 265–272.